Revue Scientifique et Technique Forêt et Environnement du Bassin du Congo
Volume 5. P. 10-21, Octobre (2015)

A Contribution to the Study of Entandrophragma Cylindricum Sprague and Lovoa Trichilioïdes Harms long term behaviour

Talla P. K.[1], Foadieng E.[1], Fouotsa W. C. M.[1], Fogue M.[2], Bishweka S[3]., Ngarguededjim K. E.[2], Alabeweh F. S.[1]

(1) L2MSP, University of Dschang, Cameroon / e-mail : tpierrekisito@yahoo.com
(2) LISIE, University of Dschang, Cameroon
(3) ULPL Goma, DRC

Abstract

This research work is entitled "A Contribution to the Study of Entandrophragma Cylindricum Sprague and Lovoa Trichilioïdes Harms long term behaviour". It aims at examining the mechanical behaviour of two species of tropical woods. First of all, we started with a general presentation of these species followed by a modelling of their mechanical behaviours using existing models, namely, that of Schapery, which illustrated the strong correlation between theoretical results and laboratory tests. As for the methodology, the sample is rigorously selected and the four-point bending creep test is based on the definition of Schapery's parameters. Therefore, data from the laboratory lead us to the conclusion that elastic deformation and creep rate of Lovoa Trichilioïdes Harms are somewhat higher than the same is for Entandrophragma Cylindricum Sprague at equal load duration and load level. The same happens with the plastic deformation. For the previous reasons, we finally stated that Lovoa Trichilioïdes Harms is less rigid in bending than Entandrophragma Cylindricum Sprague. These observations also permitted to confirm results of the literature review, namely (Gérard and al. 1998, Benoit 2008) according to which elasticity modulus of Entandrophragma Cylindricum Sprague is higher than that of Lovoa Trichilioïdes Harms. Analysis of the parameter's behaviours g_0, g_1, g_2 and a_σ reveals that it effectively depends on the load, thus confirming results found in the literature on biomaterials (Talla and al. 2007-2010, Foadieng and al. 2012). From the above-mentioned results, we provided some advices for the optimal exploitation of these two species of wood.

Keywords: *Entandrophragma Cylindricum Sprague, Lovoa Trichilioïdes Harms, creep, recovery, viscoelasticity, nonlinear, bending*

Résumé

L'objet de ce travail de recherche est une « Contribution à l'analyse du comportement différé de l'Entandrophragma Cylindricum Sprague et du Lovoa Trichilioïdes Harms ». C'est une investigation menée au sujet du comportement mécanique de deux essences de bois tropicaux. Pour mener à bien notre étude, nous avons procédé à une présentation générale de ces essences et à une modélisation de leurs comportements mécaniques en nous appuyant sur un des modèles existants, celui de Schapery. Modèle qui a révélé la très forte corrélation entre les résultats théoriques et les expériences de laboratoire. Du point de vue méthodologique, l'échantillon est rigoureusement sélectionné et l'essai de fluage en flexion quatre points s'appuie sur la détermination des paramètres du modèle de Schapery. Les résultats des essais de fluage ont révélé que la déformation élastique instantanée et le taux de fluage du Lovoa Trichilioïdes Harms sont sensiblement supérieurs à ceux de l'Entandrophragma Cylindricum Sprague à niveau de charge et durée de charge égale. Il en est de même pour la déformation plastique. Ceci nous a permis de noter en définitive que le Lovoa Trichilioïdes Harms est moins rigide en flexion que l'Entandrophragma Cylindricum Sprague. Ces observations ont permis de confirmer les résultats de la littérature (Gérard et coll. 1998, Benoit 2008) qui fait état de la supériorité du module d'élasticité de l'Entandrophragma Cylindricum Sprague par rapport à celui du Lovoa Trichilioïdes Harms. L'analyse du comportement des paramètres g_0, g_1, g_2 et a_σ nous a révélé qu'ils étaient bel et bien fonction de la charge ; ce qui confirme les résultats de la littérature relatifs aux biomatériaux (Talla et coll. 2007-2010, Foadieng et coll. 2012). Tout ceci nous a permis de prodiguer des conseils sur l'utilisation optimale de ces deux essences de bois.

Mots clés : *Entandrophragma Cylindricum Sprague, Lovoa Trichilioïdes Harms, fluage, recouvrance, viscoélasticité, non linéarité, flexion.*

Introduction

Exotic woods from Cameroon, generally strong, resistant and attractive, are now facing intense economical activities at the international level. Their impressive industrial qualities are appreciated worldwide and they are more and more solicited. They are generally ill-valorized although they can be used for many purposes, namely roof framing, furnishings, steel cross ties for railways, handles for tools, shipbuilding, stairs, veneers, bridges, body structures, woodworking, papermaking, shoes heels, etc.) ; however, those woods are not well exploited.

Often used in an empirical way, tropical woods are the source of many security and dimension problems, for instance, when they are used for the construction of bridges and heavy roof frames. Confronted to the requirements of competitiveness, a better knowledge and understanding of the material are necessary to master and optimise industrial processes, in order to improve the management of essential energy resources in the transformation processes. For, it is necessary to master physical and mainly mechanical properties of the wood, in such a way that it can highly contribute to the reduction of deforestation considering the durability of buildings constructed in the past. In recent years, knowledge from various research works (Schaffer 1972, Mukam 1990, Dubois 1997, Moutee 2006, Placet 2006, Talla 2008, Mvogo 2008) associated to the optimal exploitation of some wood properties permitted to complete the data bank on the differed behaviour of many wood species.

That is why this research work is similar. Thanks to this research work, we are associating our effort to that of other researchers in order to better understand these two species of wood.

1.1. Theoretical considerations

1.1.1. Theory of Flexural Deformation

Sills have a circular profile, thus contribute in reducing plastic deformations at the level of sills for solicitations close to that of the fracture load. In a four-point bending test, the tension's maximum stress is obtained in the middle of the lower face of the test glass while the compression's maximum stress is obtained in the middle of the upper face. Furthermore, in that part of the beam, the arrow indicates maximum (Pramanick and Sain 2006). Four-point bending test as compare to three-point bending test has the advantage that the sill is not located at the level of the rupture zone. In fact, this is a lack in the three-point system as the central sill can spoil the test tube and corrupt the results, leading to its earlier rupture.

The arrow f of the beam representing the maximum deformation of the beam at the centre ($\frac{L}{2}$) is presented as follows:

$$f = \frac{23\,PL^3}{1296\,EI} \qquad \textbf{Eq. 1}$$

The corresponding viscoelastic and viscoplastic deformation ε (t) for a period is calculated using one of the existing rheological models formulas.

1.1.2. Theory of Creep

The Schapery nonlinear viscoelastic theory can be derived from fundamental principles using the concepts of irreversible thermodynamics (Schapery 1966-1969 (a)-1969 (b)). The theory has been successfully applied to a variety of materials (Lou and Schapery 1970, Peretz and Weitzman 1982-1983, Hiel and al. 1983, Rochefort and Brinson 1983, Falcone 2006, Talla and al. 2007-2010, Marinucci and al. 2010). For the case of uniaxial loading at constant temperature, the Schapery theory reduces to the following single-integral expression.

$$\varepsilon(t) = g_0 D_0 \sigma(t) + g_1 \int_{0^-}^{t} \Delta D(\psi - \psi') \frac{dg_2\sigma(\tau)}{d\tau} d\tau \qquad \textbf{Eq. 2}$$

where $$\psi = \psi(t) = \int_{0^-}^{t} \frac{dt}{a_\sigma}, \qquad \psi' = \psi'(\tau) = \int_{0^-}^{\tau} \frac{dt}{a_\sigma} \qquad \textbf{Eq. 3}$$

D_0,ΔD (ψ) are initial and transient components of the linear viscoelastic creep compliance, respectively ; g_0, g_1 , g_2 , α_σ are stress-dependent nonlinearising material parameters.

In previous applications of the Schapery theory, $\Delta D(\psi)$ has been modeled using a power law approximation of the form:

$$\Delta D(\psi) = C\psi^n \qquad \textbf{Eq. 4}$$

This form was also used in the present study. In Eq. 4 both C and n are assumed to be material constants at any stress level, for a constant temperature. Substituting Eq. 4 into Eq. 2 results in:

$$\varepsilon(t) = g_0 D_0 \sigma(t) + g_1 C \int_{0^-}^{t} (\psi - \psi')^n \frac{dg_2\sigma(\tau)}{d\tau} d\tau \qquad \textbf{Eq. 5}$$

Now consider the stress history applied during a creep/ creep recovery test cycle, as illustrated in Figure 1.

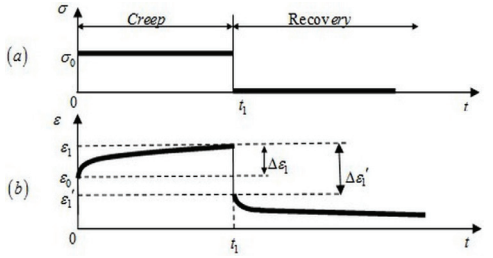

Figure 1: a) creep test followed by recovery period; b) A typical creep diagram depicting strain–time relationship.

This stress history can be expressed mathematically as:

$$\sigma(t) = \left[H(\tau) - H(\tau - t_1)\right]\sigma_0 \qquad \textbf{Eq. 6}$$

Substituting this expression into Eq. 5 results in the following equations for strain response during creep and recovery respectively:

$$\varepsilon_c(t) = g_0 D_0 \sigma_0 + g_1 g_2 C \sigma_0 \left(\frac{t}{a_\sigma}\right)^n, \qquad 0 < t < t_1 \qquad \textbf{Eq. 7}$$

$$\varepsilon_r(t) = \frac{\Delta\varepsilon_1}{g_1}\left[(1+\lambda a_\sigma)^n - (\lambda a_\sigma)^n\right], \qquad t > t_1 \qquad \textbf{Eq. 8}$$

where $\Delta\varepsilon_1$ is the total amount of strain accumulated during the creep process defined as follows:

$$\Delta\varepsilon_1 = \varepsilon(t_1) - \varepsilon_0 = g_1 g_2 C \sigma_0 \left(\frac{t_1}{a_\sigma}\right)^n \qquad \textbf{Eq. 9}$$

and λ is the non-dimensional reduced time as shown by the following:

$$\lambda = \frac{t - t_1}{t_1} \qquad \textbf{Eq. 10}$$

Equation 7 is the Schapery equation for creep, and is applicable for times $0 < t < t_1$. The values of g_0, g_1, g_2 and ασ are dependent upon the applied creep load σ_0. The instantaneous response at time *t=0* will be of interest in the following discussion. From Eq. 7 the instantaneous response to the creep load (at time *t=0*) is calculated as:

$$\varepsilon_0 = g_0 D_0 \sigma_0 \qquad \textbf{Eq. 11}$$

In the literature, Schapery has presented the recovery equation (during times) in the form of Eq. 8.

An interesting consequence of the Schapery theory involves the instantaneous change in strain following removal of the creep load at time t_1. If the recovery strain predicted immediately after t1 (calculated using Eq. 8) is subtracted from the creep strain predicted immediately before t_1 (calculated using Eq. 7), the following expression is obtained:

$$\Delta\varepsilon(t_1) = g_0 D_0 \sigma_0 + (g_1 - 1) g_2 C \sigma_0 \left(\frac{t}{a_\sigma}\right)^n = \varepsilon_0 + (g_1 - 1)\frac{\Delta\varepsilon_1}{g_1} \qquad \textbf{Eq. 12}$$

The instantaneous response to the creep load has already been shown to be Eq. 11. Thus, the instantaneous change in strain following removal of the creep load at time t_1 equals the instantaneous response at time *t*=0 only if the material is linear, i.e., if $g_1=1$. If $g_1>1$, then $\Delta\varepsilon(t_1) > \varepsilon_0$, and the resulting nonlinear recovery curve is "flatter" than the corresponding linear recovery curve. If $g_1 < 1$, then $\Delta\varepsilon(t_1) < \varepsilon_0$ and the nonlinear recovery curve is "steeper" than the linear recovery response (Tuttle and Brinson 1985).

1.2. Experimental measurement of the Schapery Parameters

The above presentation has indicated that to characterize the behaviour of a viscoelastic materials using the Schapery theory, seven material parameters are required. These are the elastic compliance term D_0, the power law parameter C, the power law exponent *n*, and the four nonlinearizing functions of stress, $g_0(\sigma)$, $g_1(\sigma)$, $g_2(\sigma)$ and $a_\sigma(\sigma)$. These parameters are customarily determined through a series of creep/ creep recovery tests at sequentially higher creep stress levels. At relatively low stress levels, linear viscoelastic behaviour is usually observed, and hence $g_0 = g_1 = g_2 = a_\sigma = 1$. Therefore, at low stress levels the Schapery single-integral (Eq. 2) reduces to the Boltzman Superposition Principle (Eq. 13). The results of the low stress level creep tests can therefore be used to determine D_0, C and *n*.

$$\varepsilon(t) = \int_{0^-}^{t} D(t-\tau)\frac{d\sigma(\tau)}{d\tau}d\tau \qquad \textbf{Eq. 13}$$

Nonlinear viscoelastic behaviour is often initiated at relatively high stress levels, and in general $g_0 \neq g_1 \neq g_2 \neq a_\sigma \neq 1$. These four parameters are determined using the results of high stress level creep tests, where it is assumed that D_0, C and n have been previously determined.

1.2.1. Linearity Region

The first step in the model characterization was to determine the region in which the behaviour was linear viscoelastic. This is necessary in order to determine the threshold stress level above which the constants g_0, g_1, g_2, and a_σ are no longer equal to one but are

dependent on the stress level. The threshold stress was determined by examining isochronous stress strain curves obtained from results of creep tests.

1.2.2. Determination of *n*, C and D_0

The first step in the characterization scheme is to define a reference recovery strain curve known as the master curve. The curve is found by comparing empirical recovery data to the predicted curve. In the linear range, assuming $g_1 = \alpha_\sigma =$ Eq. 8 reduces to the following:

$$\frac{\varepsilon_r(t)}{\Delta\varepsilon_1} = (1+\lambda)^n - \lambda^n \qquad \textbf{Eq. 14}$$

The variable n becomes the only unknown in this equation. It is determined numerically by programming equation 14. The shape of the recovery strain curve is then compared to empirical recovery data in the linear region.After the variable was determined, two more constants were determined using empirical data from the creep portion of the test. Recalling that $g_0=g_1=g_2=\alpha_\sigma=1$ in the linear range, the examination of Eq. 7 for a given creep stress level, α_σ, reveals that D_0 and C are the only unknowns:

$$\varepsilon_c(t) = (D_0 + Ct^n)\sigma_0 \qquad \textbf{Eq. 15}$$

Considering the creep strain at two different times during the creep period, $t = t_\alpha$ and $t = t_b$, where $0 < t_\alpha < t_b < t_1$, results in the following expressions:

$$\varepsilon_c(t_a) = (D_0 + Ct_a^n)\sigma_0 \qquad \textbf{Eq. 16}$$

$$\varepsilon_c(t_b) = (D_0 + Ct_b^n)\sigma_0 \qquad \textbf{Eq. 17}$$

The difference of the creep strains at $\varepsilon_C(t_\alpha)$ and $\varepsilon_C(t_b)$ becomes:

$$\varepsilon_c(t_b) - \varepsilon_c(t_a) = (t_b^n - t_a^n)C\sigma_0 \qquad \textbf{Eq. 18}$$

This equation may be solved for the unknown constant C using the experimental creep data $\varepsilon_C(t_\alpha)$ and $\varepsilon_C(t_b)$:

$$C = \frac{\varepsilon_c(t_b) - \varepsilon_c(t_a)}{(t_b^n - t_a^n)\sigma_0} \qquad \textbf{Eq. 19}$$

To provide the most accurate value, C is calculated by computing the average of all C values when t_α took on all times throughout the creep period and t_b was the time just prior to the end of the creep period. After the determination of C, it is possible to determine the initial linear viscoelastic creep compliance, D_0, from Eq. 15 as follows:

$$D_0 = \frac{\varepsilon_c(t)}{\sigma_0} - Ct^n \qquad \textbf{Eq. 20}$$

Again, the average value of D_0 was calculated for all values of t throughout the creep period. After determining the material constants *n, C*, and D_0, it is possible to plot creep and recovery strains predicted by Eq. 7 and 8 and compare the predicted strains to the empirical data used to determine these constants. Once again, $g_0 = g_1 = g_2 = \alpha_\sigma = 1$ in the linear range.

1.2.3. Determination of stress dependent constants

Next, the remaining material constants must be determined for stress levels beyond the linear range. As the instantaneous increase of strain resulting from a step increase of stress, ε_0, is known from experimental data the remaining unknown variable, g_0, may be found from Eq. 11:

$$g_0 = \frac{\varepsilon_0}{D_0\sigma_0} \qquad \textbf{Eq. 21}$$

When g_0 is known, the deformation ε_1 at the date $t=t_1$- (i.e. $\varepsilon_1(t_1\text{-}) = \varepsilon_C(t_1)$) just relief, has the following expression :

$$\varepsilon_1(t_1^-) = g_0D_0\sigma_0 + g_1g_2C\sigma_0\left(\frac{t_1^-}{a_\sigma}\right)^n = \varepsilon_0 + g_1g_2C\sigma_0\left(\frac{t_1^-}{a_\sigma}\right)^n \qquad \textbf{Eq. 22}$$

at the date $t=t_1^+$ (i.e. $\varepsilon'_1(t_1^+) = \varepsilon_r(t_1)$) just the relief, we have the following relation :

$$\varepsilon_1'(t_1^+) = g_2C\sigma_0\left(\frac{t_1^+}{a_\sigma}\right)^n \qquad \textbf{Eq. 23}$$

from Eq. 22, we have ($\Delta\varepsilon_1(t_1^-) = \Delta\varepsilon_1$):

$$\Delta\varepsilon_1(t_1^-) = \varepsilon_1(t_1^-) - \varepsilon_0 = g_1g_2C\sigma_0\left(\frac{t_1^-}{a_\sigma}\right)^n \qquad \textbf{Eq. 24}$$

In case of linear viscoelastic creep, the instantaneous elastic deformation ε_0 at the load date $t = 0^+$ is equals to the elastic recovery $\Delta\varepsilon_1'$ just after the relief at the date $t = t_1^+$. However, in the case of a non-linear viscoelastic behaviour, both deformations are different. In this case, the difference between these two deformations $\Delta\varepsilon_0$ between the dates $t = 0^+$ and $t = t_1^+$ equals to (Figure 1):

$$\Delta\varepsilon_0 = \Delta\varepsilon_1' - \varepsilon_0 \qquad \textbf{Eq. 25}$$

with

$$\Delta\varepsilon_1' = \varepsilon_1(t_1^-) - \varepsilon_1'(t_1^+) = \varepsilon_1(t_1^-) - g_2C\sigma_0\left(\frac{t_1^+}{a_\sigma}\right)^n \qquad \textbf{Eq. 26}$$

from Eq. 22 we have :

$$\varepsilon_0 = \varepsilon_1\left(t_1^-\right) - g_1 g_2 C\sigma_0\left(\frac{t_1^-}{a_\sigma}\right)^n \quad \textbf{Eq. 27}$$

Substituting Equation 26 and 27 in Equation 25, after simplifications we have:

$$\Delta\varepsilon_0 = Cg_2\sigma_0\left(g_1 - 1\right)\left(\frac{t_1}{a_\sigma}\right)^n \quad \textbf{Eq. 28}$$

Combining the equations (23) and (24), we finally deduce the expression of g_1 as follows when the plastic deformation is of minor significance:

$$g_1 = \frac{\varepsilon_1 - \varepsilon_0}{\varepsilon_1'} \quad \textbf{Eq. 29}$$

With a permanent deformation (plastic deformation) ε_p of the material, Eq. 29 becomes:

$$g_1 = \frac{\varepsilon_1 - \varepsilon_0 - \varepsilon_P}{\varepsilon_1' - \varepsilon_P} \quad \textbf{Eq. 30}$$

Determining α_σ is done numerically like in *n*. As recovery depends on Eq. 8, we have:

$$\frac{g_1\varepsilon_r(t)}{\Delta\varepsilon_1} = \left(1 + \lambda a_\sigma\right)^n - \left(\lambda a_\sigma\right)^n \quad \textbf{Eq. 31}$$

The value of α_σ is numerically found by programming Eq. 31. The process used to determine the value of g_1 is similar to that used to previously determine the constant *C*. In the non-linear range, the difference of the creep strains at t_a and t_b becomes:

$$\varepsilon_c(t_b) - \varepsilon_c(t_a) = \frac{g_1 g_2 C\sigma_0}{a_\sigma{}^n}\left(t_b{}^n - t_a{}^n\right) \quad \textbf{Eq. 32}$$

which may be solved for the quantity D_1 defined below:

$$D_1 = \frac{\varepsilon_c(t_b) - \varepsilon_c(t_a)}{\left(t_b{}^n - t_a{}^n\right)\sigma_0} = \frac{g_1 g_2 C}{a_\sigma{}^n} \quad \textbf{Eq. 33}$$

D_1 was calculated by computing the average of values of D_1 when t_a took on all times throughout the creep period while t_b was the time just prior to the end of the creep period. After determination of D_1, it is now possible to solve Eq. 33 for g_2 as follows:

$$g_2 = \frac{D_1 a_\sigma{}^n}{g_1 C} \quad \textbf{Eq. 34}$$

2. Materials and methods

2.1. Materials: Presentation of species under study

Sapelli, commercial name used for this specie of wood, is at the third position; it is also one of the species with a large exploitation volume. According to WWF (World Wildlife Fund) it is vulnerable specie, i.e. it has a high level of extinction in its natural form in the medium-term (ATIBT 2003). This specie belongs to the family of Meliaceae with the botanical name Entandrophragma Cylindricum Sprague; it is highly used for inside and outside wood trim, cabinetmaking, wood flooring, plywood, decorative veneer, shipbuilding, roof framing, bridges, bodywork, tools handles, stairs. Geographically, Entandrophragma Cylindricum Sprague is specially found in Africa, namely, in West African, Central African and East African countries (ATIBT 2003). Dibétou is the commercial name of the second specie under study, which belongs to the same family like Entandrophragma Cylindricum Sprague with the botanical name Lovoa Trichilioïdes Harms. Just like Entandrophragma Cylindricum Sprague, Lovoa Trichilioïdes Harms is only found in the African continent, that is: in West Africa and Central Africa (ATIBT 2003).

2.2. Methods

2.2.1. Preparation of test tube

The samples should have a rectangular section with straight lines as far as possible, for best and reproducible results. In this research work, all samples of Entandrophragma Cylindricum Sprague and Lovoa Trichilioïdes Harms are from the same source. Test tubes were processed taking into account the specific plane of wood for each species. The first step was to identify and find the radial and tangential direction of the wood on samples of Entandrophragma Cylindricum Sprague and Lovoa Trichilioïdes Harms. In order to determine the hygroscopy during tests, test cubes of 20 mm ridge were placed in an incubator at 103 0C following the standard NF B 51-004. Tests were carried out in the internal climatic environment of the laboratory, i.e. at an average temperature of 25 °C and air relative humidity rate of about 70 % unsaturated.

2.2.2. Experimental Setup

The test is all about a longitudinal four points bending. When, under the effect of the applied load, the test-tube is bended and has the same deformation like two well pasted strain gauges which are parallel to the axis of every test tube. The deformations are measured by Strain Bridge DELTALAB EI616 digital strain meter. During tests, temperature and relative humidity of the laboratory were given by

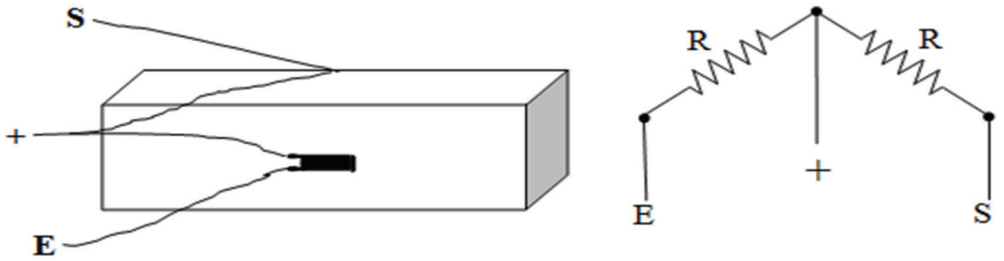

Figure 2: Construction of a half deck of Wheatstone.

an electrical thermo-hygrometer, model ETHG913R from OREGON SCIENTIFIC and a clock was used to take the time of evolution of the test tubes various deformations.

The four-point bending creep test is done following the direction which is perpendicular to fibres with the experimental layout (Talla and al. 2007-2010, Foadieng and al. 2012). The test tube with medium dimensions 340x20x20mm^3, according to the standard EN NF 408, is placed on the test stand following the longitudinal direction and the symmetry of stands. It then submitted to a constant load, lower to a third of the ultimate load to the rupture and strain ε are monitored according in the time on the strain digital bridge EI616 DELTALAB. Figure 3 shows the experimental layout:

For this stage of the research, nine levels of loads were selected: 25, 35, 50, 70, 85, 100, 115, 130 and 145 kg; this for eight test tubes of wood species. Only the test tubes presented in the following part, gave satisfactory results, for stresses from at least 35 MPa for Lovoa Trichilioïdes Harms and 47 MPa for Entandrophragma Cylindricum Sprague. At every load level, we have a series of creep tests of 10 hours; each test is followed by a phase of recovery of at least four times the creep period.

3. Results

3.1. Hygroscopy and tensile strength

Table 1 is a summary of the hygroscopy of ten references test tube for Entandrophragma Cylindricum Sprague and Lovoa Trichilioïdes Harms during tests. A series of static bending tests were done on tube tests with section-types placed on two cylindrical stands separated by a 300 mm distance and we obtained three-points tensile strengths for Entandrophragma Cylindricum Sprague and Lovoa Trichilioïdes Harms (Table 2), with the internal temperature of the laboratory at 25 °C, and a relative humidity of about 70 %.

It should be noted that determining three-point bending tensile strength stresses will permit to secure as much as possible the domain of the linear viscoelastic behaviour; it should also be noticed that four-point bending tests are carried out for stresses which are less than one third of that of three-point bending tests.

3.2. Strain-Time curves for 10-hour creep tests

Figure 4 represent an example of curve network for 10-hour of creep tests for test tube SAP1 for *Entandrophragma Cylindricum Sprague.*

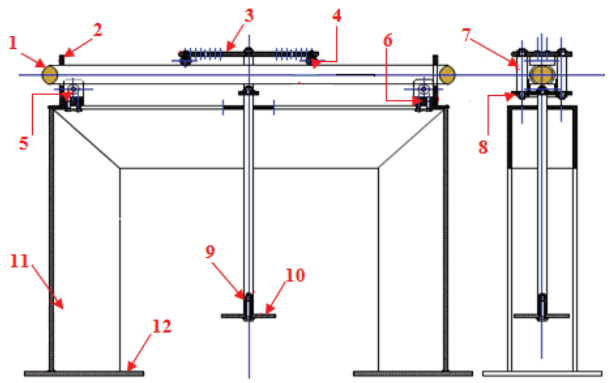

Locating	Number	Designation
1	1	Test tube
2	2	Guide
3	1	Higher support
4	2	Higher fulcrum
5	2	Lower fulcrum
6	2	Carry lower support
7	2	Pin
8	2	Lower support
9	1	Plate carries weight
10	1	Tie
11	1	Frame
12	2	Bedplate

Figure 3: Bending creep testing device and legend (Talla and al. 2010, Foadieng and al. 2012).

Table 1: Humidity H of Entandrophragma Cylindricum Sprague and Lovoa Trichilioïdes Harms kept in the laboratory under dry condition

Test tube	Entandrophragma Cylindricum Sprague			Lovoa Trichilioïdes Harms		
	mH (g)	m_0 (g)	H (%)	mH (g)	m_0 (g)	H (%)
1.	5.26	4.71	11.6	3.76	3.33	12.91
2.	5.18	4.63	11.8	3.86	3.41	13.19
3.	5.11	4.58	11.5	3.7	3.27	13.14
4.	5.34	4.77	11.9	3.97	3.51	13.1
5.	5.24	4.71	11.2	3.84	3.39	13.27
6.	5.51	4.92	11.99	4.05	3.58	13.12
7.	5.58	4.99	11.8	3.72	3.3	12.72
8.	5.29	4.74	11.6	3.99	3.52	13.35
9.	5.34	4.77	11.9	3.9	3.44	13.37
10.	5.13	4.59	11.7	3.89	3.44	13.08
Average	**5.298**	**4.741**	**11.699**	**3.868**	**3.419**	**13.125**
Standard deviation	**0.153**	**0.133**	**0.234**	**0.117**	**0.100**	**0.197**

Table 2: Load at rupture in three-point bending of Entandrophragma Cylindricum Sprague and Lovoa Trichilioïdes Harms

Test tube		1	2	3	4	5	Average	Standard deviation
Stress (MPa)	*Entandrophragma Cylindricum Sprague*	155.8	157.45	162	162	162	**149.85**	3.00
	Lovoa Trichilioïdes Harms	121.5	121.5	122.6	121.75	119.45	**120.36**	1.16

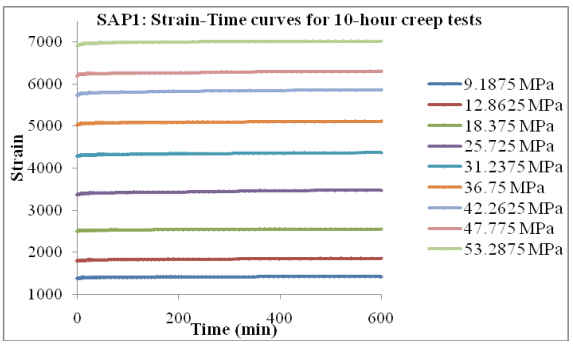

Figure 4: SAP1 Strain-Time curve network for 10-hour creep tests

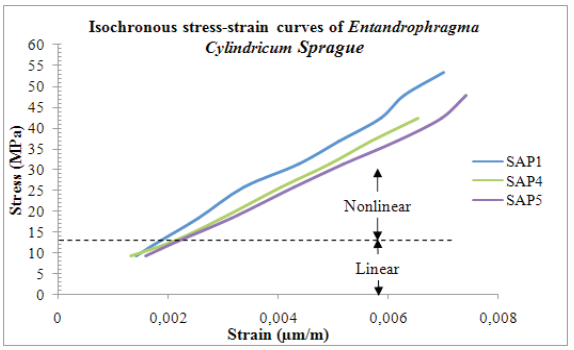

Figure 5: Isochronous stress-strain curves of Entandrophragma Cylindricum Sprague indicate region of linear viscoelastic behaviour

3.3. Schapery's model parameters

As indicated in the methodology for the determination of described parameters, we obtained the following constants n, C and D_0 on the one hand, g_0, g_1, g_2 and α_σ on the other hand. In the linear region, the threshold stress was determined by examining isochronous stress strain curves obtained from results of creep tests conducted over the stress range of 9.1875 MPa to 53.2875 MPa. As shown in Figures 5 and 6, the strain values at various times throughout each individual creep test were plotted for each stress level. In the linear region of *Entandrophragma Cylindricum Sprague* and *Lovoa Trichilioïdes Harms,* constants *n*, C and *D,* summarised in Tables 3 and 4 gave as results 12.8625 MPa and 9.1875

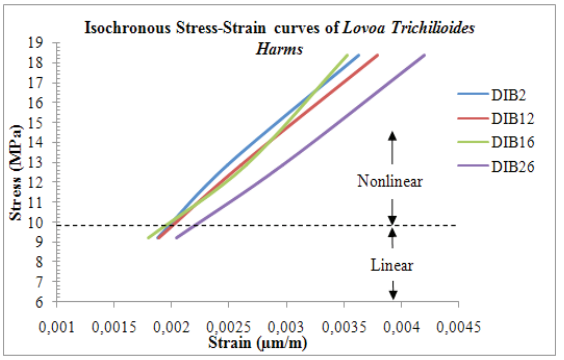

Figure 6: Isochronous stress-strain curves of Lovoa Trichilioïdes Harms indicate region of linear viscoelastic behaviour

Table 3: Parameters n, C and D_0 of Entandrophragma Cylindricum Sprague at 12.8625 MPa

Test tube	σ (MPα)	n	C	D0
SAP1		0.38	4.07×10^{-7}	1.40×10^{-4}
SAP4	12.8625	0.24	1.03×10^{-6}	1.58×10^{-4}
SAP5		0.15	3.39×10^{-6}	1.61×10^{-4}
Average		0.257	1.609×10^{-6}	1.53×10^{-4}
Standard deviation		0.116	1.573×10^{-6}	1.135×10^{-5}

Table 4: Parameters n, C and D_0 of Lovoa Trichilioïdes Harms at 9.1875 MPa

Test tube	σ (MPα)	n	C	D0
DIB2		0.59	1.94×10^{-6}	1.95×10^{-4}
DIB12		0.4	2.83×10^{-7}	2.02×10^{-4}
DIB16	**9.1875**	0.5	1.93×10^{-7}	1.91×10^{-4}
DIB26		0.33	1.10×10^{-6}	2.13×10^{-4}
Average		0.455	8.79×10^{-7}	2.003×10^{-4}
Standard deviation		**0.114**	**8.166×10^{-7}**	**9.639×10^{-6}**

MPa respectively for both species.The plots examples, shown in Figures 7 and 8, provided verification that the constants were correctly determined. It shall be noticed that the same reliability verification task were performed for other selected test tubes. Thus, we moved to the determination of the four remaining constants, namely g_0, g_1, g_2 and α_σ , as summarized in tables 5 and 6.

3.4. Comparison between experimental curves and Schapery curves

Using coefficients of Schapery theoretical prevision,

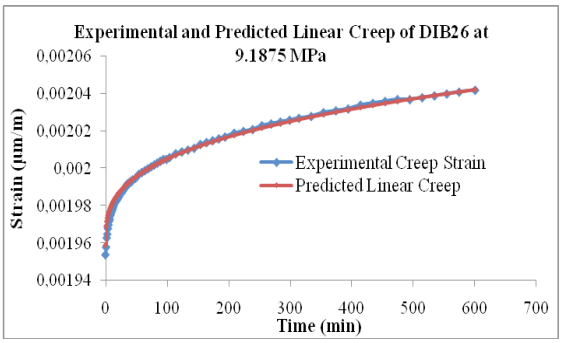

Figure 7: Experimental results of DIB26 used to determine material constants compared to predicted Creep in the linear stress range.

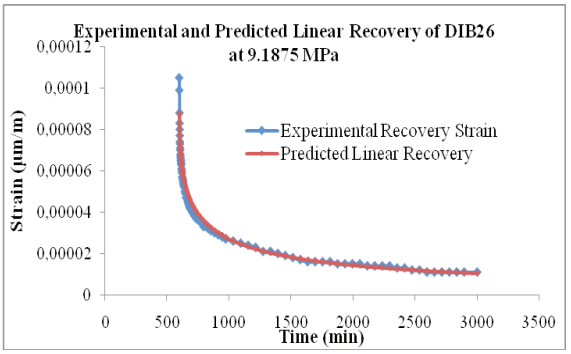

Figure 8: Experimental results of DIB26 used to determine material constants compared to predicted recovery following creep in the linear stress range

Table 5: Schapery parameters of Entandrophragma Cylindricum Sprague test tube SAP5

Test tube	σ (MPα)	g_0	g_1	g_2	α_σ
	9.1875	1	1	1	1
	12.8625	1	1	1	1
	18.375	1.190	0.936	0.454	0.200
SAP5	25.725	1.172	0.880	0.488	0.110
	31.2375	1.136	0.862	0.473	0.070
	36.75	1.157	0.851	0.544	0.140
	42.2625	1.140	0.839	0.574	0.171
	47.775	1.074	0.847	0.561	0.177

we can now compare theoretical and experimental results. On figure 9, we represented experimental and theoretical creep curves. As these parameters depend on the load, it leads us in order to make it uniform studying the variation according to it (figures 10 and 11).

Table 6: Schapery parameters of Lovoa Trichilioïdes Harms test tube DIB2

Test tube	σ (MPα)	g_0	g_1	g_2	α_σ
	9.1875	1	1	1	1
	12.8625	1.135	1.058	0.371	0.06
	18.375	1.182	0.871	0.370	0.05
DIB2	25.725	1.181	0.872	0.368	0.05
	31.2375	1.178	0.424	0.366	0.03
	36.75	1.176	1.051	0.369	0.12
	42.2625	1.138	1.244	0.368	0.02

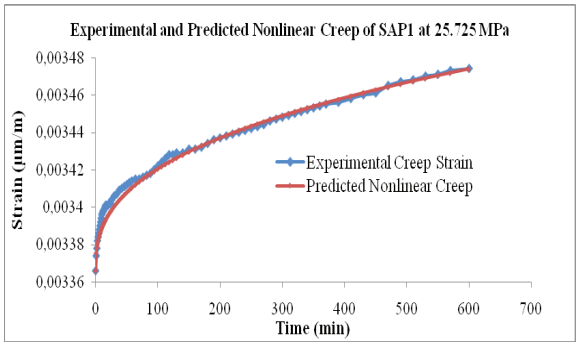

Figure 9: Comparison of the experimental data for creep with the responses of the Schapery representation of SAP1 test tube at 25.725 MPa.

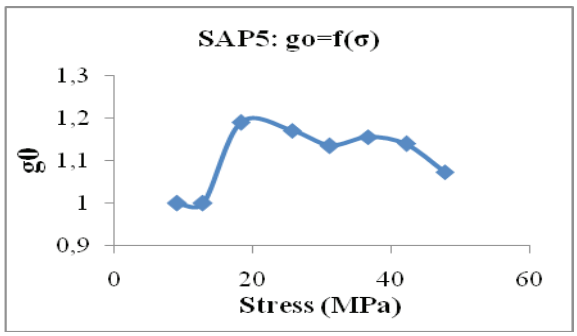

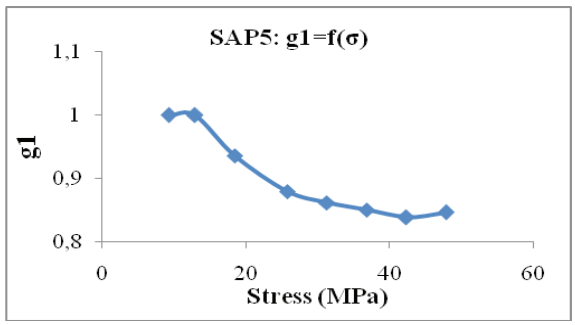

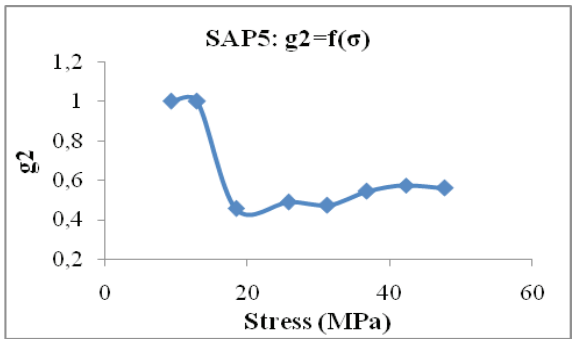

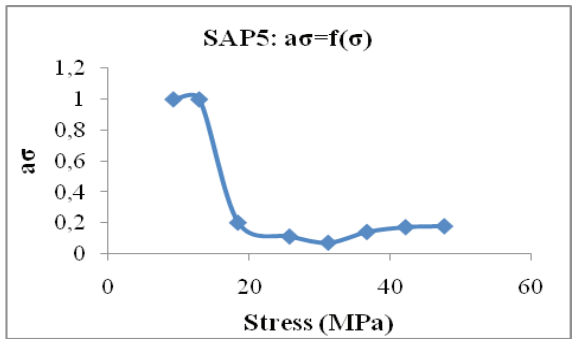

Figure 10: Curves g_0, g_1, g_2 and α_σ as functions of stress (Test tube SAP5)

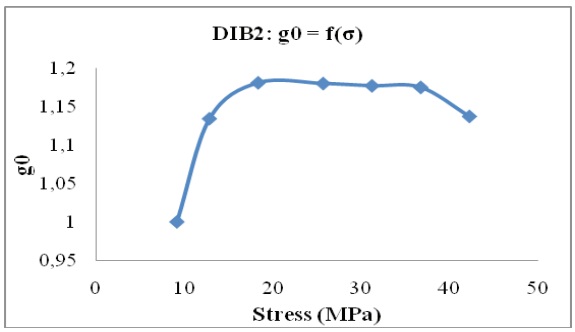

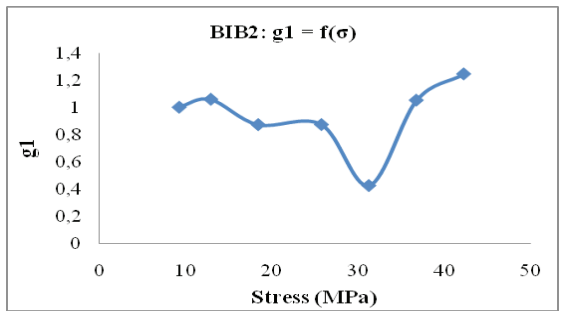

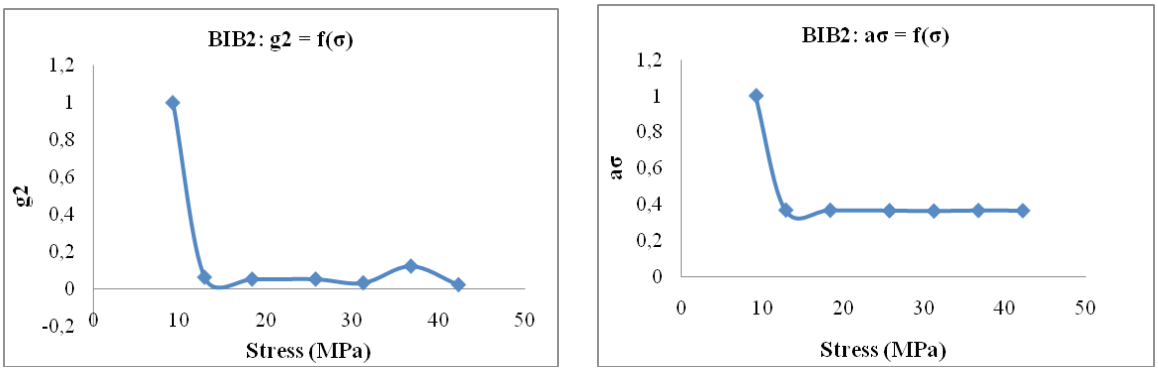

Figure 11: Curves g_0, g_1, g_2 and α_σ as functions of stress (Test tube BIB2)

4. Discussion

The hygroscopic analysis (Table 1) of our species during lab tests permitted to noticed that this humidity rate is close to 12 %, a reference value for woods comparison. Rupture tests for determining ultimate constrains in three-point bending (Table 2) show that *Entandrophragma Cylindricum Sprague* is more resistant in bending as compared to Lovoa *Trichilioïdes Harms*. Hence, we confirm results from literature (Gérard and al. 1998, Benoit 2008), reason for which this specie of wood is most of the time used for roof framing and bridges, which are mainly made to resist loads in flexion. The isochronic curves (Figure 5) of *Entandrophragma Cylindricum Sprague* are respectively showing the linear behaviour for efforts under 12 MPa and 10 MPa.

The g_0 value in general increases with stress. However, the increase is prominent only from 9.19 to 18.38 MPa, beyond that, the average g_0 value hovers at around 1.14 for *Entandrophragma Cylindricum Sprague* is and 1.17 for *Lovoa Trichilioïdes Harms*. We propose to use these values for the stress level about 18.38 MPa. The g_1 values represent the part of creep that is recoverable after the load is withdrawn. It is generally observed that the values of g_1, g_2 and a_σ decrease with the in load. However, the decrease is prominent only from 9.19 to 18.38 MPa, beyond that, the average g_1, g_2 and a_σ value respectively hovers at around 0.84, 0.55 and 1.4 for *Entandrophragma Cylindricum Sprague* is and 1.01, 0.37 and 0.05 for *Lovoa Trichilioïdes Harms*. A high value of g*1* suggests quickness in recovery. This implies that at low stress (and low strain), as the load is retracted, the recovery may behave like elastic recovery. When the value of a_σ is unity, that means the stress-related nonlinearity is a function of g_2 only.

As parameters g_0, g_1, g_2 and α_σ of Schapery model depend on the load, the high variability observed for everyone is not a new phenomenon, but a specific characteristic of materials from living organism. This can be explained by measurement and identification mistakes, position of the test tube in the tree (in fact, material characteristics of wood vary according to the position of the test tube, either on the part close to roots or in branches), non-visible blemish, possible presence of reaction woods which alter its properties. At ambient conditions of laboratory, the example of the final equation of creep in SAP5 test tube assumes the following form:

$$\varepsilon_c(t) = g_0(1.61\times10^{-4})\sigma_0 + g_1 g_2(3.39\times10^{-6})\sigma_0\left(\frac{t}{0.17}\right)^{0.15} \quad ; \quad 0 < t < t_1$$

Eq. 35

A comparative study of theoretical and experimental results (Figure 9) shows that there is a perfect agreement among those curves and this is to confirm the validity of the model used to characterize the wood material.

5. Conclusion

This research work is entitled "A Contribution to the study of *Entandrophragma Cylindricum Sprague* and *Lovoa Trichilioïdes Harms* long term behaviour". It aimed at examining the axial bending long term behaviour of two wood species. At the end of our analysis, we obtained final loads as well as the hygroscopy of *Entandrophragma Cylindricum Sprague* and *Lovoa Trichilioïdes Harms* test tubes after three-point bending tests with a constant temperature of the laboratory at about 25°C and a relative humidity rate of about 70%. Three-point bending tensile strength stresses will permit to secure as much as possible the domain of the linear viscoelastic behaviour; it should also be noticed that four-point bending tests are carried

out for stresses which are less than one third of that of three-point bending tests. We concluded after analysis of creep curves that in general, elastic strain, plastic strain and creep rate may increase according to the level of load. Furthermore, we noticed that at the same level of load and time, elastic strain, plastic strain and creep rate of *Lovoa Trichilioïdes Harms* were slightly higher than those of *Entandrophragma Cylindricum Sprague.* This result confirmed results found in the literature pointing the fact that elasticity modulus of *Entandrophragma Cylindricum Sprague* are higher than that of *Lovoa Trichilioïdes Harms*. The wood creep showed a significant stress dependency as is evident from figure 4. The compliance went up consistently with the applied stress level. These woods also showed law plasticity about 0.1-0.5 % of the total strain. The rheological model of Schapery was used to illustrate the mechanical behavior of *Entandrophragma Cylindricum Sprague* and *Lovoa Trichilioïdes Harms*. Final results were satisfactory as experimental creep curves and theoretical curves of Schapery permitted to notice that this model was in agreement with experimental data. Finally, similitude between all constraints curves of Schapery's model permitted to confirm the results.

References

ATIBT. 2003. Newsletter. N°18, 35-37. (Publication parue dans des journaux, des périodiques, des actes de congrès).

Benoit, Y., 2008. Le guide des essences de bois : 74 essences, les choisir, les reconnaître, les utiliser. Éditions Eyrolles (61, boulevard Saint-Germain, 75240 Paris cedex 05). Deuxième édition, ISBN 978-2-212- 12086-8. 145p.

Dubois, F., 1997. Modélisation du comportement mécanique des milieux viscoélastiques fissurés : Application au matériau bois. Thèse de doctorat. Spécialité : Génie Civil. Université de Limoges. Faculté des Sciences. France. 173p.

Falcone, C.M., 2006. Some aspects of the mechanical response of PMR-15 neat resin at 288 0C: Experiment and Modeling. Master of Science in Aeronautical Engineering. Air force institute of technology. Air University. 135p.

Foadieng, E., Fogue, M., Gbaguidi Aisse, G.L.,Talla, P.K., Pelap, F.B., Foudjet, A., Sinju, A. F., Bawe, G. N. and Mabekou, S.T., 2012. Effect of the span length on the deflection and the creep behaviour of Raffia bamboo vinifera L. Arecacea beam. International Journal of Materials Science. ISSN 0973-4589. Vol. 7. N° 2. pp.153–167.

Gérard, J., Edi Kouassi, A., Daigremont, C., Détienne, P., Fouquet, D. and Vernay, M., 1998. Synthèse sur les caractéristiques technologiques de référence des principaux bois commerciaux africains. CIRAD-Forêt (Campus International de Baillarguet. BP 5035, 34032 Montpellier cedex 01). France, 185p.

Hiel, C., Cardon, A.H. and Brinson, H.F., 1983. The Nonlinear Viscoelastic Response of Resin Matrix Composite Laminate. VPI&SU Report.VPI-E-83-6.

Lou, Y.C. and Schapery, R.A., 1970. Viscoelastic Characterization of a Nonlinear Fiber-Reinforced Plastic. J. Composite Materials. Vol. 5, 1971 (see also Tech. Report AFML-TR-70-113, Air Force Materials Laboratory, Wright Patterson AFB).

Marinucci, G., Farina, L.C. and Carvalho, O., 2010. Viscoelastic behaviour of carbon epoxy composites by creep tests. 14th European conference on composite materials. Budapest. Hungary ID: 544-ECCM14.

Moutee, M., 2006. Modélisation du comportement du bois au cours du séchage. Thèse de doctorat (Ph. D). Université de Laval. Faculté de Foresterie et Géomatique. Département des Sciences du bois et de la forêt. Québec. Canada. 173p.

Mukam Fotsing, J.A., 1990. Modélisation statistique du comportement mécanique du matériau bois : Application à quelques essences du Cameroun. Thèse de doctorat 3e Cycle. Spécialité : Mécanique. Université de Yaoundé. Faculté des Sciences. Cameroun. 137p.

Mvogo, J.K., 2008. Regroupement mécanique par méthode vibratoire des bois du bassin du Congo. Thèse de doctorat (Ph. D) en Sciences de l'Ingénieur. Option: Génie civil-bois. Université de Yaoundé I. École Nationale Supérieure Polytechnique. Département de Génie-Civil. Cameroun. 165p.

Peretz, D. and Weitzman, Y., 1982. Nonlinear Viscoelastic Characterization of FM-73 Adhesive. Jrnl of Rheology. Vol. 26, No 3, pg 245.

Peretz, D. and Weitzman, Y., 1983. The Nonlinear Thermoviscoelastic Characterization of FM-73 Adhesives. Jrnl of Rheology. Vol. 27, No 2. pg 97.

Placet, V., 2006. Conception et exploitation d'un dispositif expérimental innovant pour la caractérisation du comportement viscoélastique et de la dégradation thermique du bois dans des conditions sévères. Thèse de Doctorat en Sciences du Bois. Université Henri Poincaré. Nancy-I. France. 331p.

Pramanick, A.K. and Sain, M., 2006. Temperature-stress equivalency in nonlinear viscoelastic creep characterization of thermoplastic/Agro-fiber composites. Journal of Thermoplastic Composites Materials. Vol. 19. No 35. DOI: 10.1177/0892705706055443.

Rochefort, M.A. and Brinson, H.F., 1983. Nonlinear Viscoelastic Characterization of Structural Adhesives, VPI&SU Report, VPI-E-83-26.

Schaffer, E.L., 1972. Modelling the creep of wood in a changing moisture environment. Wood Fiber. Vol.3. No 4.

Schapery, R.A., 1966. A Theory of Non-Linear Thermoviscoelasticity Based on Irreversible Thermodynamics. Proc 5th U.S. National Congress Appl Mech. ASME. pg 511.

Schapery, R.A., 1969 (a). Further Development of a Thermodynamic Constitutive Theory: Stress Formulation. Purdue University Report. School of Aeronautics. AA&ES 69-2.

Schapery, R.A. 1969 (b). On the Characterization of Nonlinear Viscoelastic Materials. Polymer Engineering and Science. Vol. 9. No 4. pg 295-309.

Talla, P.K.. Pelap F.B., Fogue, M., Fomethe, A., Bawe, G.N., Foadieng, E. and Foudjet, A., 2007. Nonlinear Creep Behavior of Raphia vinifera L. (Arecacea). International Journal of Mechanics and Solids. ISSN 0973-1881. Vol. 2. N° 1. PP. 1-11.

Talla, P.K., 2008. Contribution à l'analyse mécanique de Raphia Vinifera L. Arecacea, Thèse de doctorat (Ph. D). Université de Dschang. Faculté des Sciences. Cameroun. 102p.

Talla, P.K., Foadieng, E., Fogue, M., Mabekou, J.S., Pelap, F.B., Sinju, A.F. and Foudjet, A.,2010. Nonlinear Creep Behavior of Raphia Vinifera L. Arecacea under Flexural Load. International Journal of Mechanics and Solids. ISSN 0973-1881 Vol 5, No 2. pp. 151-172.

Tuttle, M.E. and Brinson, H.F., 1985. Accelerated Viscoelastic Characterization of T300/5208 Graphite-Epoxy Laminates. NASA Contractor Report 3871. Cooperative Agreement NCC2-71.